

Analysis of the spatial distribution of stars, gas and dust in nearby galaxies

Juan Carlos Muñoz-Mateos¹

¹ National Radio Astronomy Observatory, 520 Edgemont Road, Charlottesville, VA 22903, USA, jmunoz@nrao.edu

Abstract

I summarize the main result of my thesis, which was awarded the Spanish Astronomical Society Award for the best thesis in Astronomy defended in 2010. This thesis was supervised by Armando Gil de Paz and Jaime Zamorano at Universidad Complutense de Madrid. In this work we quantified how the physical properties of stars, gas and dust vary with radius in nearby galactic disks, and used that information to infer the past assembly and evolution of galaxies. To do so we made use of spatially-resolved multi-wavelength images of nearby galaxies, all the way from the far-UV to the far-IR and radio. By comparing extinction-corrected profiles in the UV, optical and IR with models of disk evolution, we concluded that the current stellar population gradients are consistent with an inside-out growth of disks of $\sim 25\%$ since $z \sim 1$. We also found that the dust-to-gas ratio decreases with radius, and is tightly correlated with the local gas metallicity, which is again consistent with an inside-out assembly of disks. We measured the fraction of the dust mass which is in the form of PAHs at different radii. The resulting trend agrees with certain models of dust evolution, in which the abundance of PAHs is primarily determined by a delayed injection of carbon into the ISM by AGB stars.

1 Introduction

According to the Λ CDM scenario of galaxy evolution, disk galaxies are expected to grow from inside out. Due to its larger angular momentum, gas takes longer to settle onto the disk at large radii. As a result, star formation proceeds on longer timescales in the outer parts of disks, where the bulk of the stellar mass is thus assembled later. Quantifying the growth rate of disks as a function of mass is therefore a key piece in the jigsaw of galaxy assembly and evolution.

There are two different yet complementary ways to approach this problem. One consists in comparing the physical properties of galaxies at different redshifts. While this provides a

direct view of galaxy assembly, it is not always straightforward to disentangle the evolution of galaxies as individual entities from the evolution of populations of galaxies as a whole. Conversely, one can study the present-day structure of nearby galaxies, since the processes driving galaxy evolution should have left characteristic imprints on the current distribution of stars, gas and dust. For instance, if disks do indeed grow from inside out, then the star formation rate (SFR) per unit of stellar mass (also called specific SFR, or sSFR) should increase with radius, whereas the dust-to-gas ratio or the gas-phase metallicity should decrease.

In this thesis we followed the second approach, and used multi-wavelength images of nearby galaxies to constrain the current radial distribution of the physical properties of stars and the interstellar medium (ISM). We then confronted those measurements with different models to track back the temporal evolution of galaxies. The main results are summarized in the following sections; for the sake of clarity, the results have been sorted into those focusing on stellar populations and those more related to the ISM.

2 Stellar populations profiles

As explained above, radial variations in the sSFR can lead to color gradients such as those observed in nearby galaxies [11, 23, 31]. Traditionally, this kind of studies have mainly focused on optical or near-IR color gradients, but translating these into sSFR gradients is hampered by several factors. On one hand, optical data alone do not probe neither the recent star formation activity nor the old stellar populations; even when near-IR data are included, FUV data are still required to map the SFR. On the other hand, radial changes in the internal extinction can be responsible for part of the observed color gradients.

In [26] we took a step forward in this direction, and derived sSFR profiles for a sample of 161 nearby face-on disks, by performing surface photometry on GALEX FUV and NUV images [15] and on K -band ones from 2MASS [18, 19]. Besides, we corrected for the radial variation in the internal extinction, using either IRAS FIR data or calibrations based on the FUV–NUV color [7].

Figure 1 shows the sSFR gradients of our galaxies as a function of the radial scale-length of the disk in the K -band. Data-points have been also color-coded according to their absolute K -band magnitude, which is a proxy for the total stellar mass of each galaxy. Most galaxies have positive sSFR gradients and thus lie above the horizontal dashed line; in these objects, stellar populations become progressively younger, on average, as the galactocentric distance increases, consistently with the inside-out formation scenario. Conversely, a small fraction of objects present negative sSFR gradients; many of these galaxies were indeed found to exhibit central bursts of SF activity.

Interestingly, the range of observed gradients is a strong function of the mass and size of the galaxy. Low-mass disks have a wide range of sSFR gradients, mostly positive but also some negative. However, as we progress towards larger and more massive disks, the range of sSFR gradients narrows substantially, to the point the the most massive disks are characterized by almost flat but still slightly positive gradients.

We developed a simple model that mimics the expected inside-out growth of disks.

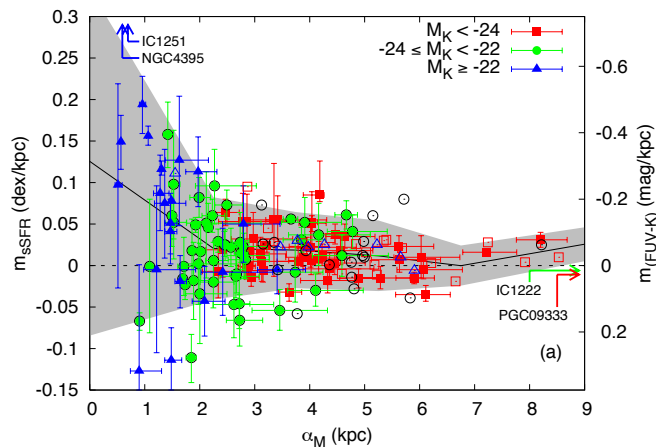


Figure 1: Specific SFR radial gradient, in dex kpc^{-1} (and the corresponding FUV– K gradient, in mag kpc^{-1}), as a function of the K -band scale-length of the disk, in kpc. Data-points are coded as a function of the absolute K -band magnitude. Open symbols correspond to galaxies with scale-lengths uncertain by more than 1 kpc. Galaxies out of range are marked with arrows. The black line and shaded area show the mean and 1σ scatter in bins of 1.5 kpc along the x -axis.

Despite its simplicity, the model is able to reproduce the basic trumpet-like distribution of Fig. 1. Our model showed that such a distribution of sSFR gradients implies an average inside-out growth of the disk scale-length of $\sim 25\%$ since $z \sim 1$. Interestingly, though, the model predicts a maximum sSFR gradient for a given size of the disk, yet we found several galaxies exhibiting much more pronounced gradients. These galaxies were independently identified by [32] as extended UV (XUV) disks. These galaxies show intense SF activity at large distances from the center, and are thought to be undergoing a phase of enhanced inside-out assembly.

In [29] we explored disk inside-out growth in more detail, by means of the models of disk evolution of [4] and [5]. These models describe the chemical and spectro-photometric evolution of galactic disks as a function of two free parameters: the maximum circular velocity of the rotation curve V_C and the dimensionless spin parameter λ . For each pair of values of V_C and λ , the models describe the gas accretion, star formation and chemical enrichment as a function of radius and time. Synthetic multi-wavelength profiles can be then built and compared with those of actual galaxies.

For this new study we made use of the *Spitzer* Infrared Nearby Galaxies Survey (SINGS, see [20]). This sample comprises 75 nearby galaxies spanning the range of morphological types and physical properties found in the Local Universe. The SINGS core dataset consists of IRAC and MIPS images that probe the spatial distribution of old stars and dust at different temperatures. This dataset is complemented by ancillary multi-wavelength images from other facilities: UV (GALEX), optical (CTIO, KPNO, SDSS), near IR (2MASS) and radio (THINGS).

We selected a subsample of 42 disks from the SINGS sample that were suitable for our analysis. While containing less galaxies than our previous sample in [26], the much richer wavelength coverage of SINGS allowed us to better constrain the star formation history at each radii. Besides, we could also better map the radial variation of the internal extinction, without resorting to indirect methods such as the FUV–NUV color (see [27]).

Figure 2 shows the observed and extinction-corrected multi-wavelength profiles of the SINGS spiral NGC 3198 (see [27, 28] for an explanation on how these profiles were obtained). This figure also shows the best-fitting disk evolution model that is able to reproduce all extinction-corrected profiles at the same time. For this particular galaxy the model yields a spin $\lambda = 0.063_{-0.010}^{+0.011}$ and a circular velocity $V_C = 191_{-5}^{+7}$ km s⁻¹. Do these values agree with the observed ones? For those galaxies with available HI rotation curves, the predicted circular velocities were found to lie within $\sim 25\%$ of the observed ones. As for the spin λ , it cannot be measured in real galaxies in such a straightforward way as V_C ; nevertheless, our values of λ follow a lognormal distribution peaking at $\lambda = 0.03 - 0.04$, in good agreement with cosmological simulations (see, e.g., [8, 34] and references therein).

Given the model’s success at fitting the multi-band profiles of our galaxies with realistic values of V_C and λ , it is safe to assume that, at least to first order, each galaxy has evolved according to the model that best fits its present-day profiles. By doing so we can then infer the typical growth rate of our disks. We found that, on average, the scale-length of disks has increased by 20–25% since $z = 1$, in very good agreement with our previous estimations [26].

These results are also consistent with observational studies at high redshift. One of the main pieces of evidence in favor of the inside-out growth of disks is the fact that the relationship between the size and stellar mass of disks is almost constant with z [1, 33]. Since the stellar mass can only increase with time, this means that the disk size must also grow accordingly.

In Fig. 3 we compare the size and stellar mass evolution predicted by the model with the observed stellar mass-size relation between $z = 0$ and $z = 1$ from [1]. As expected, the models predict that disks grow along the mass-size relation, becoming larger and more massive with time in such a way that the mass-size relation barely evolves with time.

3 Dust and gas profiles

To complement our work on the radial distribution of stellar populations in nearby disks, in [27] we carried out an exhaustive study of radial trends of the properties of dust and gas. Dust absorbs UV and optical starlight and reemits it in the IR. Therefore, in order to recover the intrinsic emission from stars one needs to be able to estimate the amount of internal extinction. The ratio between the total IR (TIR) and UV emission is known to be a robust indicator of dust attenuation [2, 24, 16, 36, 3]. By combining our GALEX and Spitzer surface photometry data, we derived radial TIR/FUV and TIR/NUV profiles for all SINGS galaxies, and converted them into extinction profiles following the prescriptions of [10], which take into account the varying dust heating of young and old stars.

We found that, in general, the internal extinction decreases with radius. It is highest

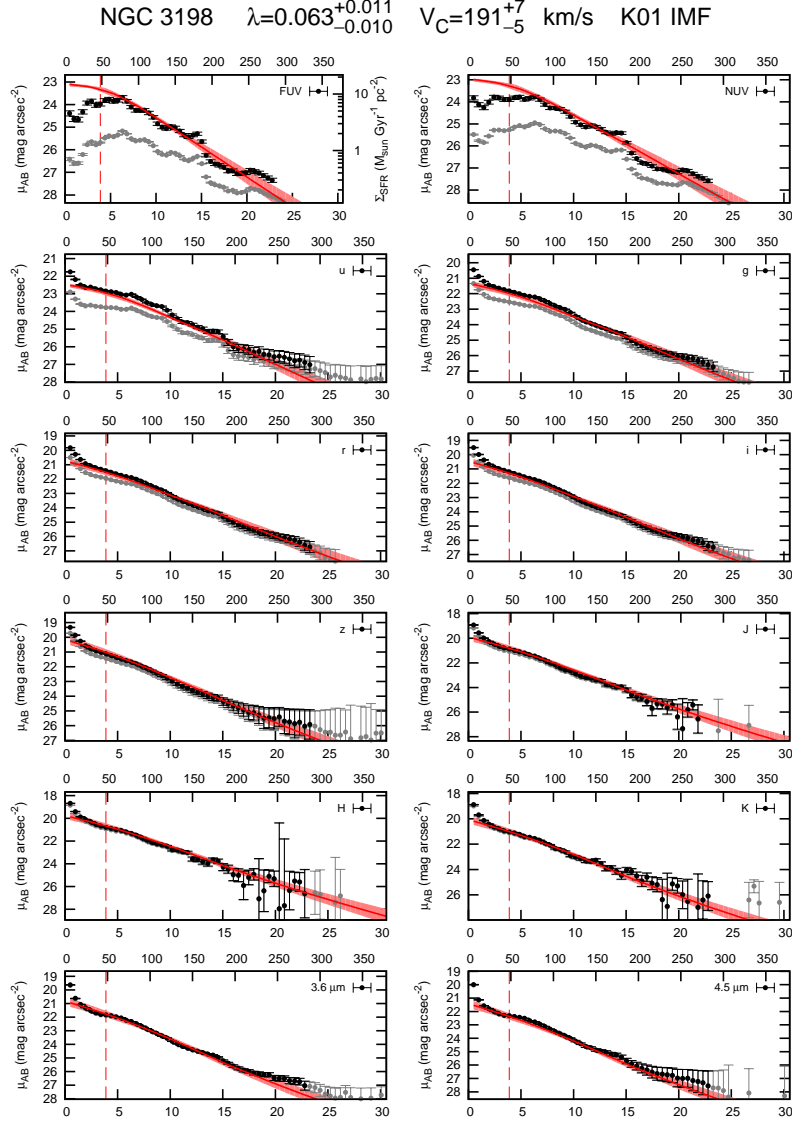


Figure 2: Observed multi-wavelength profiles and best-fitting disk evolution model for NGC 3198. The gray points show the observed data corrected for Milky Way extinction; the black ones are also corrected for internal extinction. The radius is indicated in kpc (bottom x-axis) and arcseconds (top x-axis). The red curve shows the model that best reproduces the black points at all wavelengths. The bulge-dominated region of the profile, leftwards of the vertical dashed line, is excluded from the fit. Both the model and observed profiles have been corrected for inclination. The model uses a Kroupa Initial Mass Function [22]. The best fitting values of the spin λ and circular velocity V_C are indicated on top.

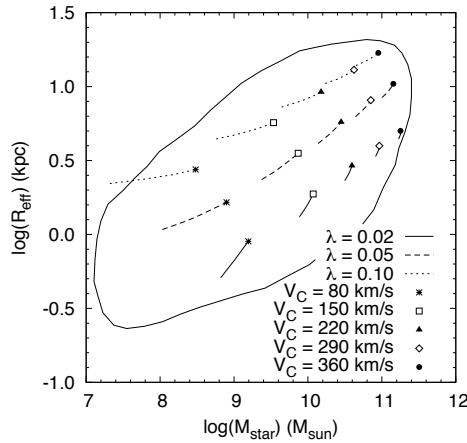


Figure 3: Evolution of the effective radius and stellar mass of model galaxies with selected values of V_C and λ . The evolution is followed from $z = 1$ to $z = 0$, the $z = 0$ step being marked with a symbol for each model. The closed curve marks the observed mass-size relation derived by [1].

in Sb-Sbc spirals, where A_{FUV} decreases from ~ 2.5 mags in the central region to ~ 1.5 mags at the optical radius of the galaxy. Sdm and irregular galaxies, on the other hand, exhibit the lowest values of internal extinction, with $A_{FUV} \sim 0.5$ mags and very weak or no radial gradient.

Since FIR data are not always available –or at least not with the desired spatial resolution–, it is convenient to have an indirect proxy for the internal extinction which does not make use of FIR data. The FUV–NUV color (or, equivalently, the slope of the UV spectrum, β) has been found to be very tightly correlated with the internal extinction in starburst galaxies, as probed by their infrared excess (IRX) over the UV light ([9, 24] and references therein). The so-called IRX– β relationship, however, cannot be applied to normal star-forming galaxies, where part of the observed UV reddening is not due to dust but to their more evolved stellar populations, compared to starburst galaxies. To circumvent this limitation, in [27] we derived an updated IRX– β relation valid for normal star-forming galaxies, using our TIR/FUV and FUV–NUV radial profiles. This relationship can be used to estimate the internal extinction in other normal star-forming galaxies for which FIR data are not available.

In order to study the spatial variation of other dust properties such as its mass, temperature or composition, we fitted our IR radial profiles with the dust models of [12]. These models describe the IR spectral energy distribution of dust as a function of four parameters: the fraction of the dust mass contributed by polycyclic aromatic hydrocarbons (q_{PAH}), the intensity of the radiation field heating the diffuse dust (U_{min}), the fraction of dust exposed to very intense starlight in photo-dissociation regions (γ) and the total dust mass (M_{dust}) or, in our case, since we are dealing with radial profiles, the dust mass surface density ($\Sigma_{M_{dust}}$). We therefore derived the radial variation of these four parameters for the SINGS galaxies.

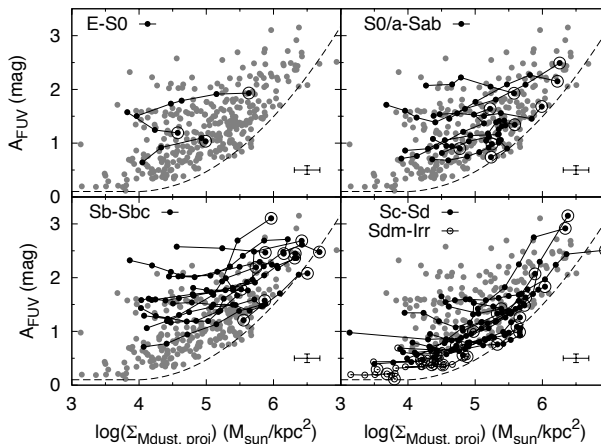


Figure 4: Internal extinction, derived from the TIR/FUV ratio, as a function of the projected dust mass surface density, from the models of [12]. Each data-point corresponds to a certain radius in each galaxy. The gray points show the whole sample, whereas the black ones correspond to galaxies of specific morphological types, as labeled in each panel. Black points belonging to the same galaxy are connected with a solid line, with the point at the center of each galaxy being surrounded by a larger circle. The dashed line shows a fit to the lower envelope of the distribution.

In Fig. 4 we plot the internal extinction, computed as explained above, as a function of the projected dust mass surface density. Each data-point corresponds to a given elliptical annulus in a certain galaxy, so that each galaxy is represented by a set of data-points at different galactocentric distances. We can clearly see that both parameters are positively correlated. However, the scatter is large, and for a given dust column density there is a wide range of observed attenuation values. More interesting is the fact that there is a very well-defined lower envelope in this distribution: for any dust surface density there is always a minimum internal extinction value. This lower envelope is nicely defined by Sc spirals and later. After a careful analysis of the dust temperature distribution in all these different regions, we concluded that this behavior most likely reflects differences in the relative distribution of stars and dust along the Hubble sequence. Dust clouds are probably clumpier and more porous in late-type disks than in early-type ones, so that the same dust column density (averaged over kpc scales) yields a lower extinction in late-type galaxies.

Another interesting result of our study concerns the spatial variation of the abundance of PAHs. These complex organic molecules are known to be scarce in low metallicity environments (see, e.g., [13] and references therein). However, the origin of this trend is unclear. Some authors favor an evolutionary origin for this trend [14]. PAHs are thought to form in the envelopes of stars in the Asymptotic Giant Branch (AGB), whereas other metals now locked in bigger dust grains are believed to form in supernovae (SN). Since AGBs evolve on longer timescales than SN, this would lead to a delayed injection of PAHs into the ISM compared to other dust species, leading to the observed paucity of PAHs in low-metallicity

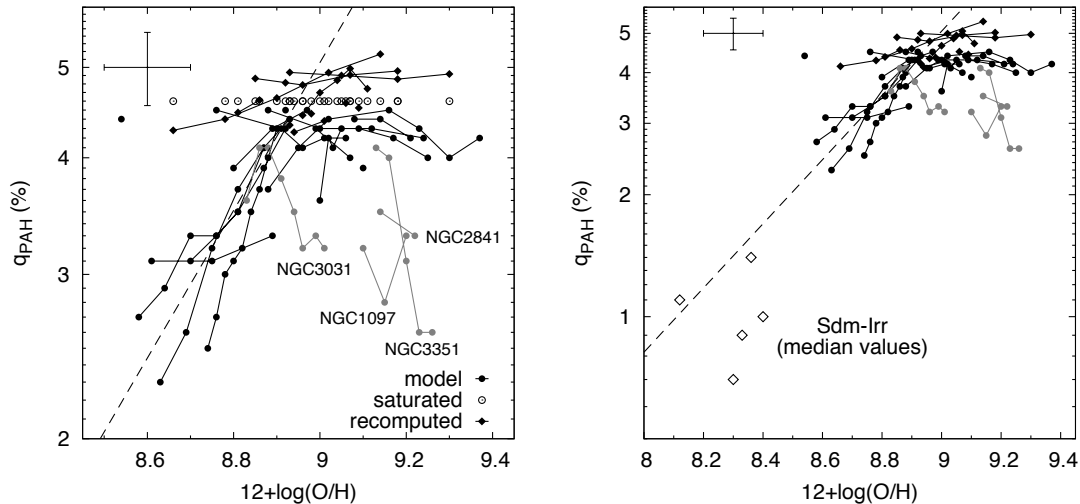


Figure 5: PAH fraction as a function of the local gas-phase metallicity, for those spiral galaxies with available O/H gradients (*left*) and including median values for dwarf irregulars (*right*). The gray points correspond to galaxies in which q_{PAH} decreases with increasing O/H (all of them early-type disks). The open circles correspond to cases in which q_{PAH} reaches the maximum value allowed by the dust models of [12]. These “saturated” values have been recomputed empirically (see [27] for details). The dashed line shows a fit to the points with metallicities below 9.0, but excluding dwarfs.

systems. Conversely, PAHs may be selectively destroyed by the harsh radiation field in low-metallicity regions, due to both a relatively larger fraction of young OB stars and a lower level of shielding by dust. Indeed, a trend between PAH spectral features and the radiation field hardness has been reported (see, e.g., [30] and references therein).

In Fig. 5 we show the abundance of PAHs as a function of the local oxygen abundance at each radius, for those galaxies with available metallicity profiles from [25]. The left panel only includes spiral galaxies, whereas the right one shows dwarf irregulars as well (only median values are used for these galaxies, since no O/H profiles were available for them). We can reproduce the overall trend of increasing PAH abundance with increasing metallicity reported by previous authors. However, using radial profiles reveals an interesting behavior: at large metallicities, the trend flattens and even reverses. This is consistent with the predictions of the dust evolution models of [14], in which this effect is due to the fact that AGBs with different masses (or lifetimes) and metallicities have a different carbon content.

This seems to support the idea that, at least at kpc scales, the observed trend between the PAH fraction and the gas-phase metallicity is partly driven by evolutionary effects. This

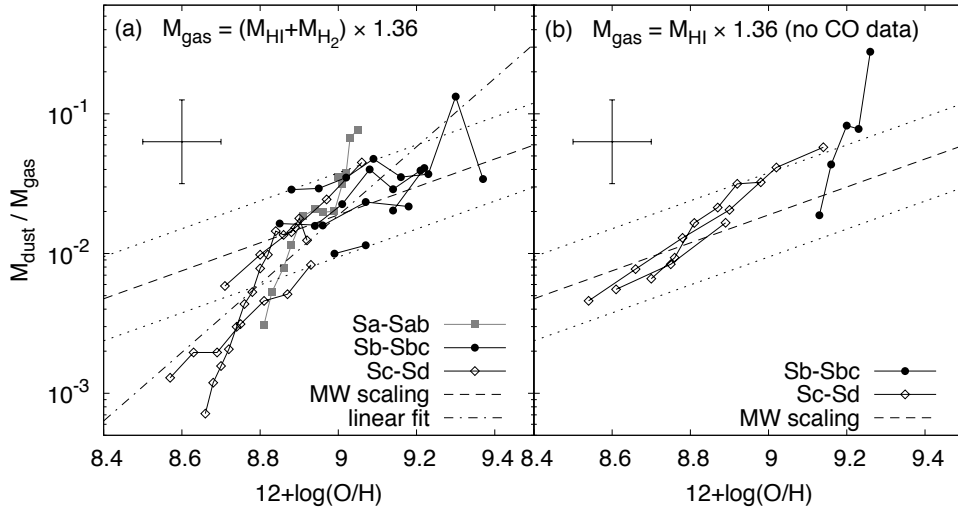


Figure 6: Dust-to-gas ratio as a function of the local oxygen abundance at different radii. Galaxies in panel (a) are those for which H_2 profiles were available in the literature; those in panel (b) did not have such data, and their DGRs are thus upper limits. Different symbols correspond to different morphological types. The dashed line shows a linear (1:1) scaling relation between DGR and O/H, with a factor of ± 2 indicated by the dotted lines. The dash-dotted line is a fit to the data, $DGR \propto (O/H)^{2.45}$.

is without prejudice to the fact that PAHs may be indeed destroyed at smaller scales, in star-forming regions with locally hard radiation fields. Also, note that even in the diffuse ISM the abundance of the different dust species is not just determined by the rate at which they were produced and injected there: it also depends on the different processes of dust growth, destruction and re-growth that take place later in the ISM itself.

Another key property of the ISM that allows us to investigate the assembly and evolution of galactic disks is the dust-to-gas ratio (DGR), which is expected to increase as time goes by and the interstellar gas becomes more metal rich. A positive correlation between DGR and O/H has been indeed found when studying the integrated properties of galaxies ([13] and references therein). If disks do indeed grow from inside out, we would expect DGR to decrease with galactocentric distance, since the outskirts of disks are assembled over longer timescales. For many years, however, spatially resolved studies of DGR in external galaxies were limited to a handful of objects [17, 6].

To shed further light in this topic, in [27] we presented DGR profiles for a large subset of the SINGS galaxies. To do so, we combined our dust mass profiles with HI profiles from The HI Nearby Galaxies Survey (THINGS, [35]) and, whenever possible, with H_2 profiles compiled from different sources. Figure 6 shows the resulting DGR profiles as a function of the local oxygen abundance at each radius. We can clearly see that DGR decreases with metallicity, and is thus lower in the outer parts of disks. This trend is fully consistent with an inside-out assembly of galactic disks, with outer disks being less chemically evolved.

In the high-metallicity regime, the DGR follows a linear trend with metallicity: to first order, the DGR of a given region can be predicted within a factor of 2 by simply scaling the local DGR in the Milky Way with the corresponding metallicity. However, the metal-poor outer regions of late-type disks appear to have lower DGR than what is expected for their metallicities. While the presence of cold dust –poorly constrained by the MIPS 160 μm data– could partly account for this deficit, such low DGRs could also imply that the physics of star and dust formation are significantly different in the outer parts of disks.

4 Multi-wavelength morphology

Galaxy morphology constitutes an invaluable tool to study galaxy formation and evolution. However, the traditional Hubble classification scheme is not very well suited for many modern surveys. On one hand, performing a visual classification on samples of several thousands or millions of galaxies is clearly impractical. On the other hand, the classical Hubble types cannot fully grasp the wealth of morphological features that we observe at UV or FIR wavelengths, or in high- z galaxies.

Numerical morphological estimators, with their own disadvantages, overcome all these limitations. Some of the most common estimators are the concentration index, the asymmetry, the second order moment of the brightest 20% of the pixels, and the Gini coefficient. In [28] we computed all these estimators for all SINGS galaxies, in more than 20 bands from the FUV to the FIR. Such a dataset constitutes a very useful local benchmark to study galaxy morphology at higher z .

5 Conclusions

In this work we have shown that the present-day radial distribution of stars, gas and dust in nearby galaxies provides invaluable clues on the processes governing galaxy assembly and evolution. The current gradients of stellar populations in nearby disks are consistent with an average increase of 20%–25% in the scale-length of disks since $z = 1$. Similarly, radial gradients in properties of the ISM such as the dust-to-gas ratio also point towards an inside-out formation scenario.

Acknowledgments

I would like to thank my thesis advisors, Armando Gil de Paz and Jaime Zamorano, for their sincere advice and constant support. My gratitude is extended to the members of the Astrophysics Department in Complutense University, as well as the many co-authors of the papers that constitute this thesis, for their invaluable help. I was funded by a FPU fellowship from the Spanish Ministry of Education and Science, as well as several grants from the Spanish National Program of Astronomy and Astrophysics awarded to our research group over the years. I would also like to thank the GALEX, 2MASS, SINGS and THINGS teams for making such a valuable dataset available to the community; I am particularly grateful to F. Walter and A. Leroy for sharing their THINGS HI profiles.

References

- [1] Barden, M., Rix, H.-W., Somerville, R. S., et al. 2005, *ApJ*, 635, 959
- [2] Buat, V. & Xu, C. 1996, *A&A*, 306, 61
- [3] Buat, V., Iglesias-Páramo, J., Seibert, M., et al. 2005, *ApJ*, 619, 51
- [4] Boissier, S. & Prantzos, N. 1999, *MNRAS*, 307, 85
- [5] Boissier, S. & Prantzos, N. 2000, *MNRAS*, 312, 398
- [6] Boissier, S., Boselli, A., Buat, V., Donas, J., & Milliard, B. 2004, *A&A*, 424, 465
- [7] Boissier, S., Gil de Paz, A., Boselli, A., et al. 2007, *ApJS*, 173, 524
- [8] Bullock, J. S., Dekel, A., Kolatt, T. S., et al. 2001, *ApJ*, 555, 240
- [9] Calzetti, D., Kinney, A. L., & Storchi-Bergmann, T. 1994, *ApJ*, 429, 582
- [10] Cortese, L., Boselli, A., Franzetti, P., et al. 2008, *MNRAS*, 386, 1157
- [11] de Jong, R. S. 1996, *A&A*, 313, 377
- [12] Draine, B. T., & Li, A. 2007, *ApJ*, 657, 810
- [13] Draine, B. T., Dale, D. A., Bendo, G., et al. 2007, *ApJ*, 663, 866
- [14] Galliano, F., Dwek, E., & Chianial, P. 2008, *ApJ*, 672, 214
- [15] Gil de Paz, A., Boissier, S., Madore, B. F., et al. 2007, *ApJS*, 173, 185
- [16] Gordon, K. D., Clayton, G. C., Witt, A. N., & Misselt, K. A. 2000, *ApJ*, 533, 236
- [17] Issa, M. R., MacLaren, I., & Wolfendale, A. W. 1990, *A&A*, 236, 237
- [18] Jarrett, T. H., Chester, T., Cutri, R., et al. 2000, *AJ*, 119, 2498
- [19] Jarrett, T. H., Chester, T., Cutri, R., Schneider, S. E., & Huchra, J. P., 2003, *AJ*, 125, 525
- [20] Kennicutt, R. C., Jr., Armus, L., Bendo, G., et al. 2003, *PASP*, 115, 928
- [21] Kong, X., Charlot, S., Brinchmann, J., & Fall, S. M. 2004, *MNRAS*, 349, 769
- [22] Kroupa, P., 2001, *MNRAS*, 322, 231
- [23] MacArthur, L. A., Courteau, S., Bell, E., & Holtzman, J. A. 2004, *ApJS*, 152, 175
- [24] Meurer, G. R., Heckman, T. M., & Calzetti, D. 1999, *ApJ*, 521, 64
- [25] Moustakas, J., Kennicutt, R. C., Jr., Tremonti, C. A., et al. 2010, *ApJS*, 190, 233
- [26] Muñoz-Mateos, J. C., Gil de Paz, A., Boissier, S., et al. 2007, *ApJ*, 658, 1006
- [27] Muñoz-Mateos, J. C., Gil de Paz, A., Boissier, S., et al. 2009b, *ApJ*, 701, 1965
- [28] Muñoz-Mateos, J. C., Gil de Paz, A., Zamorano, J., et al. 2009a, *ApJ*, 703, 1569
- [29] Muñoz-Mateos, J. C., Boissier, S., Gil de Paz, A., et al. 2011, *ApJ*, 731, 10
- [30] Smith, J. D. T., Draine, B. T., Dale, D. A., et al. 2007, *ApJ*, 656, 770
- [31] Taylor, V. A., Jansen, R. A., Windhorst, R.A., et al. 2005, *ApJ*, 630, 784
- [32] Thilker, D. A., Boissier, S., Bianchi, L., et al. 2007, *ApJS*, 173, 572

- [33] Trujillo, I., Forster, S., Natascha, M., et al. 2006, *ApJ*, 650, 18
- [34] Vitvitska, M., Klypin, A. A., Kravtsov, A. V., et al. 2002, *ApJ*, 581, 799
- [35] Walter, F., Brinks, E., de Blok, W. J. G., et al. 2008, *AJ*, 136, 2563
- [36] Witt, A. N. & Gordon, K. D. 2000, *ApJ*, 528, 799